PRELIMINARY EVALUATION OF CESIUM ATOMIC FOUNTAIN NICT-CsF2

Motohiro Kumagai, Clayton R. Locke, Hiroyuki Ito, Masatoshi Kajita, Yuko Hanado and Mizuhiko Hosokawa

National Institute of Information and Communications Technology,
4-2-1 Nukui-Kitamachi, Koganei, Tokyo 184-8795, Japan
E-mail: *mkumagai@nict.go.jp*

Abstract

NICT in Japan is developing a cesium atomic fountain NICT-CsF2 with the goal of operation at the 10^{-16} level. It is the second atomic fountain to be constructed at NICT and it shares many features with the first fountain NICT-CsF1. A narrow Ramsey signal of less than 1Hz has been observed and the short-term stability is currently $3\times10^{-13}/\tau^{1/2}$. An evaluation of systematic frequency shifts and their uncertainties has commenced and preliminary results are presented here.

INTRODUCTION

The atomic fountain clock **[1]** is a technology that currently provides the best realization of the SI second and provides support to the development of next-generation optical frequency standards. Several state-of-the-art fountain clocks at major international institutions around the world make a collaborative effort in the calibration of the global atomic timescale (TAI.)

NICT has long played an important role in contributions to the international atomic time scale, beginning with the magnetically state-selected type CRL-CS1 in 1987 **[2]** and the optically pumped NICT-O1 in 2004 **[3]**. The first atomic fountain developed at NICT (CsF1) developed in 2006 **[4]** with accuracy at the 10^{-15} level not only contributed to the accuracy of TAI but also was responsible for improving Japan Standard Time (JST) **[5]**.

The construction of a second fountain clock was fuelled by dual purposes. Firstly, a second fountain clock allows vital evaluation between fountains, frequency shifts and uncertainties. The relative frequency instability of the difference frequency between two fountain clocks in the same laboratory averages down according to the square root of the measurement time, and has been shown **[6]** to reach $2\text{x}10^{-16}$ at 50,000 s. Secondly, another fountain clock will provide redundancy necessary for guaranteed contribution to TAI.

The opportunity was taken with the construction of this second fountain to implement several design changes and improvements, detailed in the next section. We present preliminary evaluation of frequency shifts and the uncertainty budget of this newly operational fountain clock.

SYSTEM DESCRIPTION

DESIGN OF NICT-CSF2

The design of NICT-CsF2 is shown in Figure 1, consisting of, in ascending order, a laser cooling region, a detection region, and a microwave interaction region. Although similar to NICT-CsF1, a significant difference between the two is the laser cooling configuration; CsF2 adopts a (1,1,1) laser cooling geometry enabling large diameter cooling beams to irradiate and capture many atoms without a magnetic gradient. (In the conventional (0,0,1) configuration the cooling beam diameter is limited by the aperture of the microwave cavity.) Capture by pure optical molasses reduces the atomic number density and thus reduces the collisional shift, this being especially critical as it is the dominant source of frequency uncertainty in NICT-CsF1. A conventional rectangular cavity for state-selection is installed just above the laser cooling region (about 8cm above the loading point). The resonant mode is TE_{102} with a loaded quality factor of approximately 100.

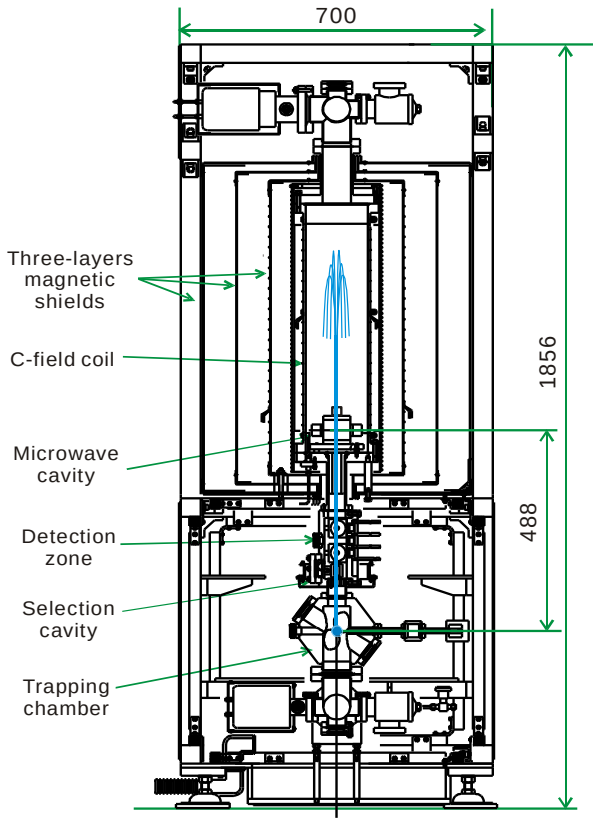

Figure 1. Physical package structure of NICT-CsF2.

The C-field coil in the flight tube is 70 cm long and 20 cm in diameter, capped at either end by additional coils 6 cm long used to improve the magnetic uniformity throughout the atoms' flight. The microwave cavity used for the Ramsey interaction has a radius of 28 mm and a height of 23.2 mm, and has quarter-wave chokers to suppress the unwanted TM_{111} mode. The microwave frequency Ramsey signal is fed into the cavity through two equally balanced couplings on opposite sides in order to create a uniform field distribution. The atoms enter through holes at top and bottom end-caps which have 5cm long cut-off tubes to prevent the microwave leaks. The offset is adjusted to be below 1 MHz without detuning

with the temperature control. The loaded quality factor is about 18,000. This microwave interaction region is surrounded by three layers of molly permalloy magnetic shielding, yielding a shielding factor of order 10^3.
The detection chamber of CsF2 is the same as that of CsF1; it has three laser interaction areas where the falling atoms are irradiated by the detection laser, and post processing of these signals allows normalization between flight-to-flight measurements. Two pairs of spherical mirrors of diameter 20 mm are mounted at the highest and the lowest ports, focusing the fluorescence light onto a large active area (1 cm^2) Si photodetector via a light pipe. The port between upper and lower detection zones is used for optical pumping of the atoms in the $F = 3$ state to the $F = 4$ state.

Graphite tubes mounted between the laser cooling region and the detection region, and between the detection region and the microwave interaction region, work as absorbers that prevent inflow of excessive Cs vapor into the microwave interaction region. Despite the possibility of these carbon materials in the chamber limiting ultra high vacuum, we have been able to achieve less than 2×10^{-8} Pa in the microwave interaction region using two ion pumps and two non-evaporable getter (NEG) pumps.

The total height of the NICT-CsF2 is 1.8 m, and the distance between the loading point and the microwave cavity is 49 cm. The chambers of the laser cooling region and the detection region are made of stainless steel (316L) and that of the microwave interaction region is made of aluminum. The microwave cavities and the spherical mirrors are made of oxygen-free copper. Great care was taken not to use magnetic components in the microwave interaction region.

OPTICAL SETUP

An external-cavity diode laser is used as a master laser in NICT-CsF2. The lasing frequency is stabilized to the Cs D_2 $F = 4$ - $F' = 5$ saturated absorption line by modulation transfer spectroscopy technique where only the pump beam is modulated by an external 16 MHz electro-optic modulator and the Pound-Drever-Hall-like error signal is fed back to the piezo actuator and the laser current of the ECDL. Careful temperature control of the Cs cell used to obtain the D_2 line allows many weeks of uninterrupted operation. The stabilized ECDL light is sent through an acousto-optic modulator (AOM), which shifts the laser frequency of order 100 MHz before entering a 500 mW taper amplifier (TA). To produce the required several hundred mW of power necessary for laser cooling, the TA requires an input of a few tens of mW. Importantly, the output power fluctuation of the TA is highly sensitive to fluctuations of the input power. To overcome this problem we have employed an injection-locking technique, whereby a 100 mW single-mode diode laser is installed between the AOM frequency shifted master laser and the TA. Any input power fluctuations are filtered out before the TA - including those changes induced by AOM as its frequency is shifted over 30MHz.

The output beam from the taper amplifier is split into two beams, their frequency and the power intensity independently controlled with double-passed AOMs. The beams are coupled into polarization maintaining fiber and then further split into 3 beams, resulting in the 6 beams required for laser cooling. A portion of the slave laser is used for the detection beam.

Another ECDL stabilized to the $F = 3 – F' = 2$ transition by the same technique is used to provide a repump beam and is injection-locked to another slave laser. Using AOMs, the laser frequency is tuned to the $F = 3$ - $F' = 4$ transition to pump the $F = 3$ atoms back to the $F = 4$ state. All AOMs are synchronized to less than 3 μs using a direct digital synthesizer (DDS), and mechanical shutters eliminate residual laser light. All laser beams are delivered to the vacuum chamber through polarization-maintaining fiber and the beams are

linearly polarized and launched into free space with a collimated diameter of 25 mm and having a power density of greater than 10 mW/cm^2.

MICROWAVE SOURCE

The performance of a primary frequency standard (fountain clocks included) is often limited by the short term stability of its reference local oscillator (LO). In fact, the performance of NICT-CsF1 was limited by the frequency instability of the hydrogen maser used as a LO **[4]**. Recently NICT has acquired a cryogenic sapphire oscillator (CSO), developed at the University of Western Australia, having a short term frequency stability about 100 times better than a hydrogen maser. It is based on a high-quality cylinder of HEMEX single-crystal sapphire in which the resonant modes of the electromagnetic field are located along the inside circumference in a so-called Whispering Gallery formation. The sapphire cylinder is enclosed in a silver-plated copper cavity and temperature- controlled inner vacuum can for isolation from environmental perturbations. An outer can encloses the inner can and microwave components, and is then immersed in a liquid helium bath. The sapphire crystal, kept slightly above liquid helium temperature, has a high unloaded quality factor of about 10^9, working as an ultra narrow bandpass filter and dispersive element in a Pound frequency stabilization scheme. Details are described in Ref. **[7, 8]**.

The NICT CSO oscillates at 11.2005 GHz, with a short-term stability better than 2×10^{-15} at an averaging time of 1 second. In order to make the most of this highly stable signal for several experiments in several different laboratories within NICT, it is necessary to develop a synthesis chain to change to the appropriate frequency without any drastic degradation of the frequency stability. For laboratory distribution, we firstly use a synthesis chain to down-convert from 11.2005 GHz to 1 GHz, which is then distributed to other experimental rooms via coaxial cable.

Figure 2(a) shows the block diagram of the 1 GHz down-converter. The output signal of a 1 GHz low-noise surface acoustic wave (SAW) oscillator is amplified and injected into a nonlinear transmission line. The nonlinear transmission line is used for frequency multiplication as a frequency comb generator. The 11th harmonic (11 GHz) is bandpass filtered and mixed with the 11.2005 GHz output from the CSO to generate a 200.5 MHz signal. The 5th harmonic (5 GHz) from another nonlinear transmission line is divided to 208.3 MHz by divide-by-eight and divide-by-three pre-scalars. The 208.3 MHz signal is mixed with the 200.5 MHz to generate 7.8 MHz. Fine tuning of the down-converter is achieved by controlling a commercial direct digital synthesizer (DDS) in the chain. The zero beat between the two 7.8 MHz signals at the last mixer is used to phase-lock the 1 GHz SAW oscillator to the CSO. The intermediate signal (200 MHz) in the down-converter is mixed with a doubled 100 MHz signal from the hydrogen maser in order to compensate the long-term frequency drift dependence of the CSO. By this slow stabilization, the frequency difference between the output signal from the down-converter and the hydrogen maser becomes zero, making it traceable to Japan Standard Time (JST) and International Atomic Time (TAI).

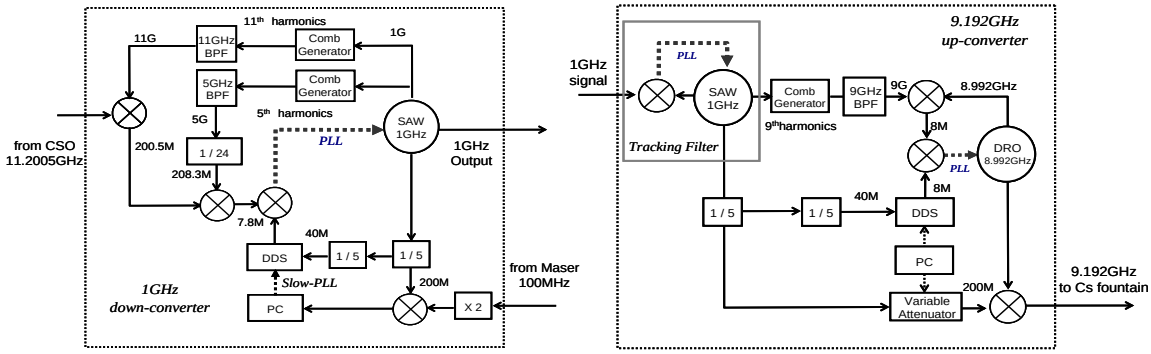

Figure 2(a) Block diagrams of the 1GHz down-converter and (b) of the 9.192GHz up-converter.

A 9.192 GHz microwave signal is required for interrogation of the Cs atoms, generated from the 1 GHz signal using an up-converter as shown in Figure 2(b). Firstly, the distributed 1 GHz is phase-locked to a 1 GHz SAW oscillator, providing a stable amplitude source for the synthesis chain. The 1 GHz output signal from the SAW oscillator is amplified and injected into a comb generator. The 9th harmonic (9 GHz) of the comb is filtered by means of the bandpass filter and mixed with the 8.992 GHz output from a dielectric resonant oscillator (DRO) to generate 8 MHz. The fine tuning of the up-converter is achieved by controlling a DDS in the chain. The zero beat between the down-converted 8 MHz and the 8 MHz output from the DDS is used to digitally phase-lock it to the 8.992 GHz DRO. A portion of the 8.992 GHz output is mixed with 200 MHz to generate a 9.192 GHz signal.

Two nominally identical frequency converters are assembled to evaluate the performance of the converters themselves. By measuring the residual frequency stabilities of down converter and up-converter shown in Figure 3, we have confirmed that both converters do not degrade the frequency stability of the input signal. Using the CSO as an ultra stable flywheel oscillator and this frequency down-and up-conversion technique, we can then use it to interrogate atoms in the NICT fountain clocks. We have seen an improvement in the short term stability of NICT-CsF1, and we have now utilized it on NICT-CsF2.

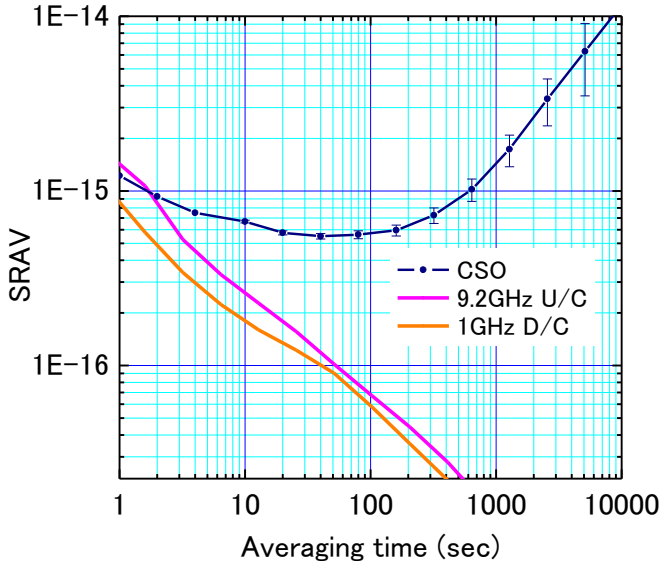

Figure 3. The short-term stability of the cryogenic sapphire oscillator and the residual frequency instabilities of frequency converters for the CSO.

FOUNTAIN OPERATION

DATA ACQUISITION

NICT-CsF2 operates in cyclic process which consists of the following steps; loading atoms by the pure optical molasses, launching upward and sub-Doppler cooling, state-selection of the $m_F = 0$ component, optical blasting of $m_F \neq 0$ components, two Ramsey interactions separated by a flight time, and normalized detection (observation of the transition probability). The operation cycle lasts approximately 1.68 sec.

At the beginning of the launch process cesium atoms are captured by optical molasses (the number of captured atoms by optical molasses is 10 times less than that by MOT). The pre-cooled atoms are launched upward by a (1, 1, 1) moving molasses, in which the downward and upward vertical beams are detuned by -2.7 MHz and +2.7 MHz, respectively. The launched atoms are post-cooled to a few μK by polarization gradient cooling (PGC). In the PGC stage, the intensities of cooling laser beams are reduced slowly and their detuning from the optical resonance are gradually increased from 10 MHz to 50 MHz. Finally, all laser beams are turned off using AOMs and fully extinguished by mechanical shutters.

In the selection cavity, the $m_F = 0$ components of the launched atoms ($F = 4$) are pumped to the ($F = 3$, $m_F = 0$) state by a π-pulse microwave. Those atoms remaining in the $F = 4$ state are blasted away by the radiation pressure of the blasting beam, which in CsF2 is the detection beam as experienced by atoms on their upward path. The ($F = 3$, $m_F = 0$) atoms continue the ballistic flight into the Ramsey cavity. Two π/2-pulses are applied, the first as the atoms pass up and the second pulse as they return down, giving rise to the Ramsey resonance. The signal is normalized by measuring both the number of atoms in the $F = 4$ state and also

those in the $F = 3$ state. The fraction $P = N_4 / (N_4 + N_3)$ yields the normalized transition probability, free from the influence of the cycle-to-cycle fluctuation of the number of launched atoms.

Given an initial velocity of 4.1 m/s the atoms are launched to an apogee 36 cm above the microwave cavity, which gives the drift time (time duration between the first and the second Ramsey interactions) T_r of 526 msec. As a result, the Ramsey fringe is narrower than 0.95 Hz. The observed Ramsey fringe is shown in Figure 4(a). Figure 4(b) shows the Ramsey signals including $\Delta m_F = 0$ transitions of $m_F \neq 0$ components and $\Delta m_F = \pm 1$ transitions of $m_F = 0$ component.

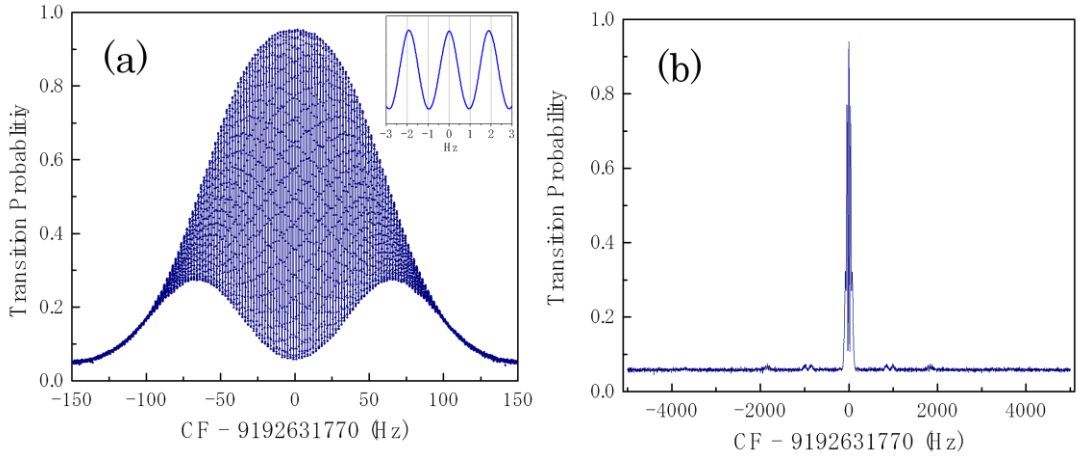

Figure 4. (a) Observed Ramsey fringe pattern of the clock transition in CsF2. (b) Observed Ramsey signals including $\Delta m_F = 0$ transitions of $m_F \neq 0$ components and $\Delta m_F = \pm 1$ transitions of $m_F = 0$ component.

FREQUENCY STABILITY

The LO frequency derived from the CSO is locked to the Ramsey resonance by a frequency modulation locking method, in which the LO frequency is toggled between $f_0 - \delta\nu/2$ and $f_0 + \delta\nu/2$ where f_0 is the central microwave frequency, and $\delta\nu$ is the line width of the Ramsey fringe. The central frequency f_0 is then controlled to make the signal intensities at the two toggled frequencies equal. This is achieved by steering the output frequency of the DDS in the 9.2 GHz up-converter, and the amount of steering is proportional to the difference in fraction P at the two frequencies. The Dick effect **[9]** has been calculated to be negligible due to the use of the ultra stabile CSO reference. The short-term stability of the CsF2 is limited only by the number of the atoms interacting with the microwave field inside the Ramsey cavity. Figure 5 shows the Allan deviation of the frequency difference between NICT-CsF2 and the CSO reference. A preliminary frequency stability of $3.1 \times 10^{-13}/\tau^{1/2}$ has been achieved.

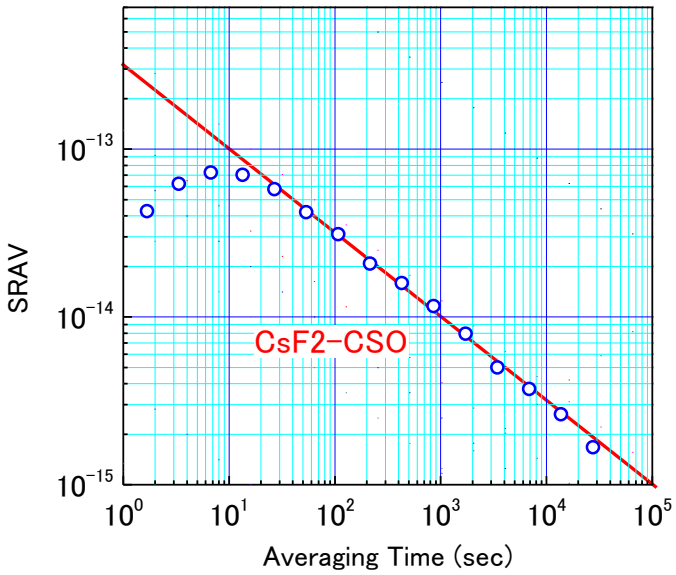

Figure 5. Allan deviation of the CsF2 against the reference based on the CSO.

SYSTEMATIC FREQUENCY SHIFTS AND THEIR UNCERTAINTIES

Owing to the long Ramsey interaction time, the frequency shifts due to systematic effects in atomic fountains are much smaller than those of thermal beam-type standards. Consequently, their uncertainties are also smaller. All of the frequency shifts and their uncertainties in NICT-CsF2 are evaluated theoretically and experimentally. Some systematic shifts are evaluated by making the most of the high frequency stability of CsF2; however, the long-term drift of the reference often makes precise evaluation difficult and requires repeat measurements. We adopt an interleaved measurement approach where two or more data sets are obtained independently and consecutively. Although the frequency stability degrades due to the longer operation cycle time between comparable data acquisitions, this technique avoids the influence of the drift of the reference in estimations of the small or negligible biases like collisional shifts, light shifts, etc. We can also directly compare CsF2 with CsF1 for precise evaluations of both long and short term stability

Evaluations of systematic frequency shifts and their uncertainties of the CsF2 have commenced. Table 1 shows preliminary evaluation results of the frequency shifts in CsF2. Most of them have been completed, although a few systematic shifts need further evaluation. After all evaluations are complete a detailed evaluation report will be published.

Table 1. Systematic frequency biases and their uncertainty budgets of NICT-CsF2.

Physical Effect	Bias	Uncertainty
2nd Zeeman	298.27	0.05
Collision		
Blackbody Radiation	-15.50	0.10
Gravity Potential	8.36	0.05
MW-power dependence		
Cavity Pulling	0.0	0.02
Rabi Pulling	0.0	<0.01
Ramsey Pulling	0.0	<0.01
AC Stark		
Distributed cavity phase		
Spectral impurities	0.0	0.01
Majorana	0.0	0.01
Background Gas	0.0	0.10
units are fractional frequency x10^{-15}		

SUMMARY

NICT is developing a second cesium atomic fountain NICT-CsF2 to complement its existing operating fountain NICT-CsF1. The captured atoms in the optical molasses are launched upward by a (1,1,1) moving molasses with a reduced collisional shift owing to the reduced atomic density. An initial velocity of 4.1m/sec gives a drift time of 526 msec and we have observed a Ramsey signal of width 0.95Hz. A microwave reference based on a cryogenic sapphire oscillator is locked to the center of the Ramsey fringes and currently short-term frequency stability is $3.1\times10^{-13}/\tau^{1/2}$. An evaluation of all of the systematic frequency shifts and their uncertainties of the CsF2 has commenced and preliminary results presented.

REFERENCES

[1] R. Wynands and S. Weyers, 2005, *"Atomic fountain clocks,"* **Metrologia, Vol. 42,** S64-S79.

[2] K. Nakagiri, M. Shibuki, H. Okazawa, J. Umezu, Y. Ohta, and H. Saitoh, 1987, *"Studies on the accurate evaluation of the RRL primary cesium beam frequency standard,"* **IEEE Transactions on Instrumentation and Measurement**, **IM-36**, 617-619.

[3] A. Hasegawa, K. Fukuda, M. Kajita, H. Ito, M. Kumagai, M. Hosokawa, N. Kotake, and T. Morikawa, 2004, *"Accuracy evaluation of optically pumped primary frequency standard CRL-O1,"* **Metrologia, Vol. 41**, 257-263.

[4] M. Kumagai, H. Ito, M. Kajita, and M. Hosokawa, 2008, *"Evaluation of caesium atomic fountain NICT-CsF1,"* **Metrologia**, **Vol. 45**, 139-148.

[5] Y Hanado, K. Imamura, N. Kotake, N. Nakagawa, Y. Shimizu, R. Tabuchi, L.Q. Tung, Y. Takahashi, M. Hosokawa, and T. Morikawa, 2008, *"The new generation system of Japan Standard Time at NICT,"* **International Journal of Navigation and Observation**, 841672.

[6] S. Bize, P. Laurent, M. Abgrall, H. Marion, I. Maksimovic, L. Cacciapuoti, J. Grünert, C. Viana, F. Pereira dos Santos, P. Rosenbusch, P. Lemonde, G. Santarelli, P. Wolf, A. Clairon, A. Luiten, M. Tobar, and C. Salomon, 2004, *"Advances in atomic fountains,"* **Comptes Rendus Physique**, **Vol. 5**, 829.

[7] S. Chang, A.G. Mann, and A.N. Luiten, 2000, *"Improved cryogenic sapphire oscillator with exceptionally high frequency stability,"* **Electronics Letters**, **Vol. 36**, 480-481.

[8] C. R. Locke, E. N. Ivanov, J. G. Hartnett, P. L. Stanwix, and M. E. Tobar, 2008, *"Design techniques and noise properties of ultrastable cryogenically cooled sapphire-dielectric resonator oscillators,"* **Review of Scientific Instruments, Vol. 79**, 051301.

[9] G. J. Dick, 1987, *"Local Oscillator Induced Instabilities in Trapped Ion Frequency Standards,"* Proceedings of the Annual PTTI System and Application Meeting, pp. 133-47.